Growth of long fatigue cracks under non-proportional loadings – experiment and simulation

Y. Hos, M. Vormwald
Technische Universität Darmstadt, Materials Mechanics Group, Franziska-Braun-Straße 3 64287 Darmstadt/GERMANY
hos@wm.tu-darmstadt.de, vormwald@wm.tu-darmstadt.de

ABSTRACT. An experimental campaign was carried out on thin-walled tubes under tension and torsion. The results from experiments are measured and compared. It is observed that cracks follow a shear-dominated growth pattern with increasing crack length, instead of a tension-dominated one. The experiments are performed with high amplitudes applied to the specimens, resulting in large cyclic plastic deformations and crack growth rates up to 10^{-3} mm/cycle. Stress intensity factors were calculated for the proportional loading case.

KEYWORDS. Multiaxial fatigue; Non-proportional loadings; Crack growth; Fracture mechanics; Experimental mechanics; Numerical simulation

INTRODUCTION

Fatigue crack growth under non-proportional mixed-mode loading depends on many factors. A recently issued review [1] identified seven such factors. The first one, mode-mixity, is arguably the most obvious one. The maximum tangential stress criterion has been supported by several experimental results [2-4], whereas Roberts and Kibler [5] have discovered cases where maximum shear stress criterion is more suitable. Natural mode I cracks were produced firstly, and then loaded with mode II loading, without observing a change in the direction of the crack. Only the maximum shear stress criterion can model this behavior. It could be concluded that increasing mode-mixity leads to a tendency for a shear-dominated crack growth. Secondly, the material itself is a dominant factor. For example, Qian and Fatemi [2] conclude that "mode II crack growth occurs more often in aluminum alloys than in steels". Thirdly, the magnitude of cyclic plastic deformation is an influencing factor, as increasing cyclic plastic deformation creates a tendency towards shear-dominated crack growth. Results published by Tanaka [6], Brown and Miller [7], Otsuka and Tohgo [8], Socie [9] and Doquet and Bertlino [10] support this argument. The fourth factor to be specified is the crack closure, which is directly dependent on the cyclic plastic deformation. Roughness along the crack front leads sometimes to the interlocking of the crack fronts, and interlocking results in a shielding of the crack tip from mode II (especially in low stress intensity factor ranges). Moreover, the mean stress effect (the fifth factor) is very relevant to the crack closure and therefore needs to be taken into account. In addition, the geometry of a structure is obviously a very important factor in every type of crack growth phenomenon. Finally, the mode-mixity changes along the crack front in three-dimensional cases.

With so many plastic effects playing a role in crack growth under non-proportional loading, a crack tip parameter, which takes plasticity into account, has to be used in further research. Several studies [11-15] have shown that ΔJ is a very

successful parameter to model fatigue crack growth under proportional and non-proportional loadings, therefore an opportunity might arise to extend this solution to long cracks. The ΔJ-integral should be interpreted according to the definitions of Dowling and Begley [16], Wüthrich [17] and Hertel et al. [18]. However, short cracks usually grow in a single plane without significant kinks or curvature, so the modeling could be simplified to an iterative search of this plane. More about the plastic simulations can be found in [19, 20].
A research project was launched on the abovementioned basis, seeking further knowledge on the mechanisms. This paper covers the achievements of this project. The investigation embarked on high amplitude loading, accompanied by large cyclic plastic deformation, high crack growth rates and short fatigue lives, and the cracks being all naturally produced.

DESCRIPTION OF THE PROBLEM

Constant amplitude fatigue tests have been performed on thin-walled tubes which were put under either uniaxial tension-compression load, or torsional load, or a combination of both (proportional and non-proportional). The specimen geometry is depicted in Fig. 1. Longitudinally welded tubes were sawed and the starter notch was machined onto the specimen. The centers of holes at the ends of the starter notch are 10 mm apart from each other (length of an arc at the outer surface). The notch was positioned opposite to the weld.

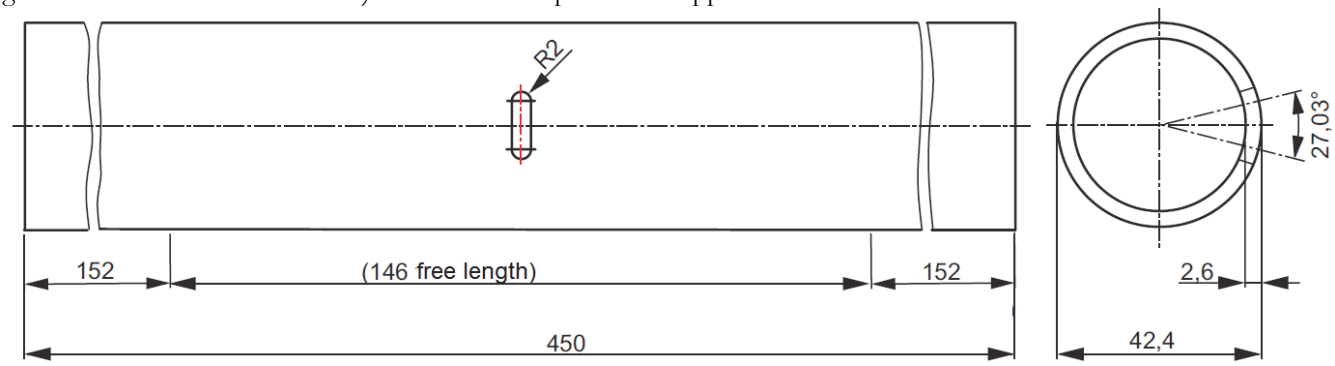

Figure 1: Specimen geometry

Inducing cyclic plastic deformation was a primary goal in the experiments. For this purpose, the tubes were ordered to be manufactured from the low strength constructional steel S235. The experimental results are shown in Fig. 2. The blue points in Fig. 2 correspond to strain-controlled tests and they show the upper end of the hysteresis at each strain level, measured at half-life each. A more detailed discussion of material properties could be found in previous works of the authors. [19, 20, 25, 26].

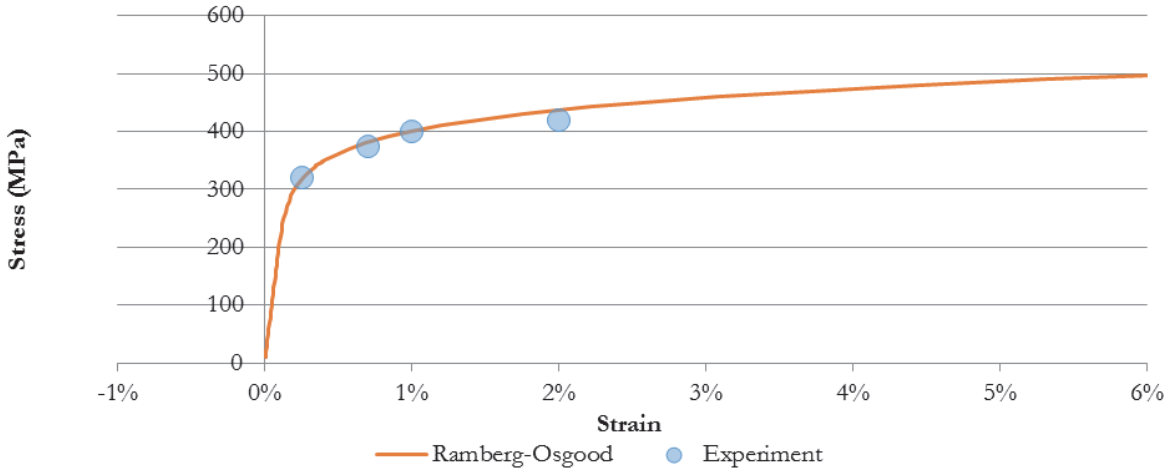

Figure 2: Cyclic stress-strain curves of the used material.

E in MPa	$R_{p0.2}$ in MPa	K' in MPa	n'
210000	378	680	0.11

Table 1: Mechanical properties of S235

Two different types of crack growth experiments were performed. In the first series of experiments, photos of the specimen were taken during experiment at predefined intervals. (Length of the interval is dependent on the nature of the experiment) Three cameras were installed in front of the starter notch, one facing the notch directly, the second with a 45° angle to the right and the third with a 45° angle to the left. After a certain number of cycles, the experiment was stopped, and a load corresponding to 90% of the maximum cyclic load was applied. During the short hold time, the photos of the specimen surface were taken. The specimen was unloaded again and the cyclic loading continued. The pictures were evaluated after the experiment, with the help of the laser-engraved dot pattern on the surface.
Five different loading sequences were used in the experiments: pure tension-compression loading, pure torsion loading, proportional loading resulting from the superposition of these two and out-of-phase loading with phase angles of 45° and 90°. The experiments were conducted under load/moment control, using a servo-hydraulic, four-pillar tension-torsion machine, with frequencies ranging between 0.25 Hz and 2 Hz. A temperature of 21°C and a relative air humidity of 50% were kept constant.
The cracks were assumed to be through-wall cracks with a straight crack front. The crack length is defined as the arc length, where the crack starts at the crack initiation location in each test. The scheme of the presentation of the results in references [20] and [22] were taken as a guide, with crack 1 being left and crack 3 being right. In the second series of experiments, the tests were interrupted in the fashion that was described above, only this time, the whole cycles were recorded and analyzed applying the digital image correlation (DIC) technique. More details about DIC can be found in references [19] and [20]. Later, the results of this analysis are utilized while dealing with crack closure in the simulations.

EXPERIMENTAL RESULTS

Uniaxial Tension-Compression Loading

The specimen R-002 was tested uniaxially with a cyclic tension-compression force (F_{max} = 35 kN and R_F = -1). Two symmetric cracks grew in the centre cross-section, check Fig.3. The crack growth curve was indicated in Fig. 4.

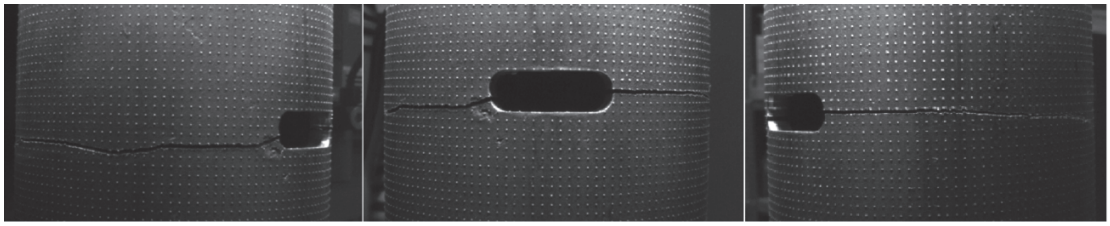

Figure 3: Cracks in the specimen R-002, pure tension-compression with F_{max} = 35 kN and R_F = -1, steel S235.

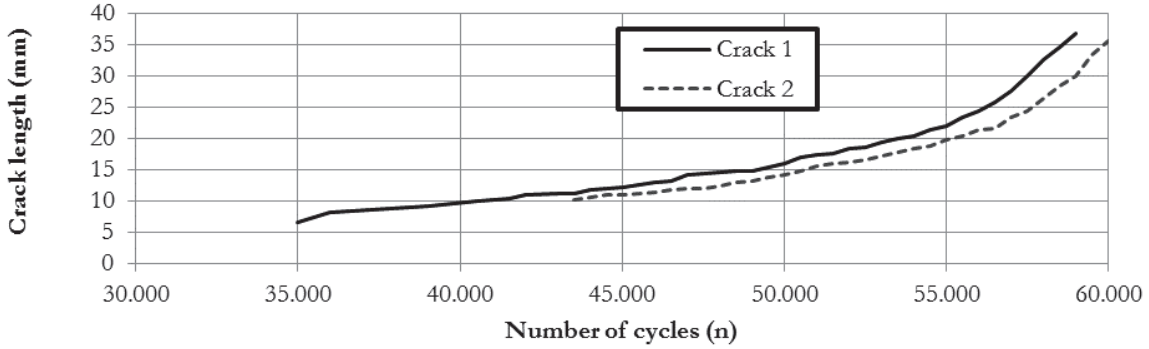

Figure 4: Crack growth curve of specimen R-002, pure tension-compression with F_{max} = 35 kN and R_F = -1, steel S235.

Multiaxial Loading

Three types of multiaxial loading were conducted: proportional loading, 90° out-of-phase loading and 45° out-of-phase loading, namely the specimens R-004, R-005 and R-006 respectively. The amplitudes of the loadings are F_{max} = 33 kN, M_{max} = 382 Nm and $R_F = R_M$ = -1. The nominal stresses in the gross section corresponding to these loads are $\sigma_{n,max}$ = 101.5 MPa and $\tau_{n,max}$ = 62.6 MPa. Again two cracks were initiated at the notch. The different crack paths can be seen in Figs. 5-7 with a summary in Fig. 8.

The crack growth directions in Fig. 5 are inclined 17° and 18° to the cross-section plane, respectively for crack 1 and 3. Some cyclic mode II loading is expected to have contributed to the fatigue crack growth. This argument was discussed with more detail in the forthcoming chapters about simulation.

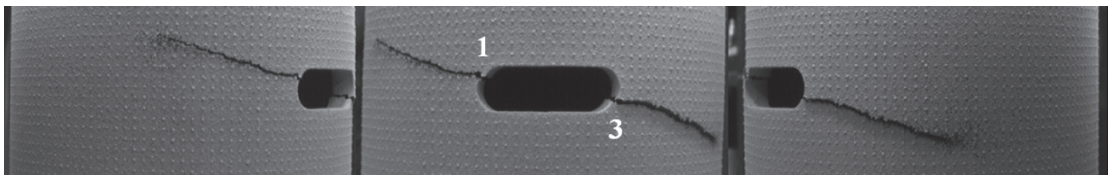

Figure 5: Cracks in specimen R-004, proportional loading with F_{max} = 33 kN, M_{max} = 382 Nm and $R_F = R_M$ = -1, steel S235.

After putting a 90° phase shift between the two loadings, the cracks stopped growing symmetrically, as shown in Fig. 6. Crack 1 grew straight, with an angle of 45° approximately to the specimen axis, and after a crack length of 17 mm, the crack changes direction to a direction perpendicular to the specimen axis, and soon after that the specimen fails.

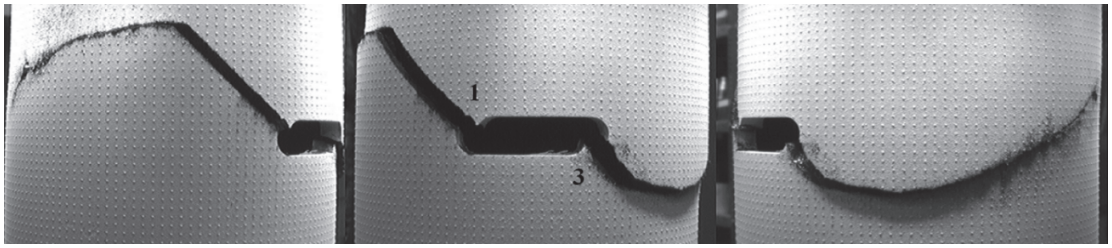

Figure 6: Cracks in specimen R-005, 90° out-of-phase non-proportional loading with F_{max} = 33 kN, M_{max} = 382 Nm and $R_F = R_M$ = -1, steel S235.

Last but not least, the specimen, which was loaded with 45° out-of-phase loading, was shown in Fig. 7. Crack 1 had a kink quite early, but crack 3 continued linearly, and after some time, it made a kink too. Crack 1 continued in a zigzag pattern after the kinking, which leads to an argument that the crack cannot decide between two options and switches back and forth continuously. Fig. 8 shows a comparison of these three cracks and this zigzag pattern is more obviously visible.

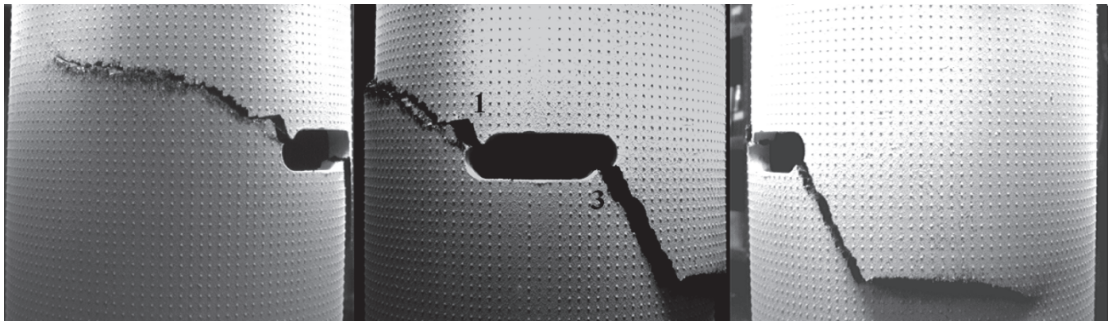

Figure 7: Cracks in specimen R-006, 45° out-of-phase non-proportional loading with F_{max} = 33 kN, M_{max} = 382 Nm, $R_F = R_M$ = -1, steel S235.

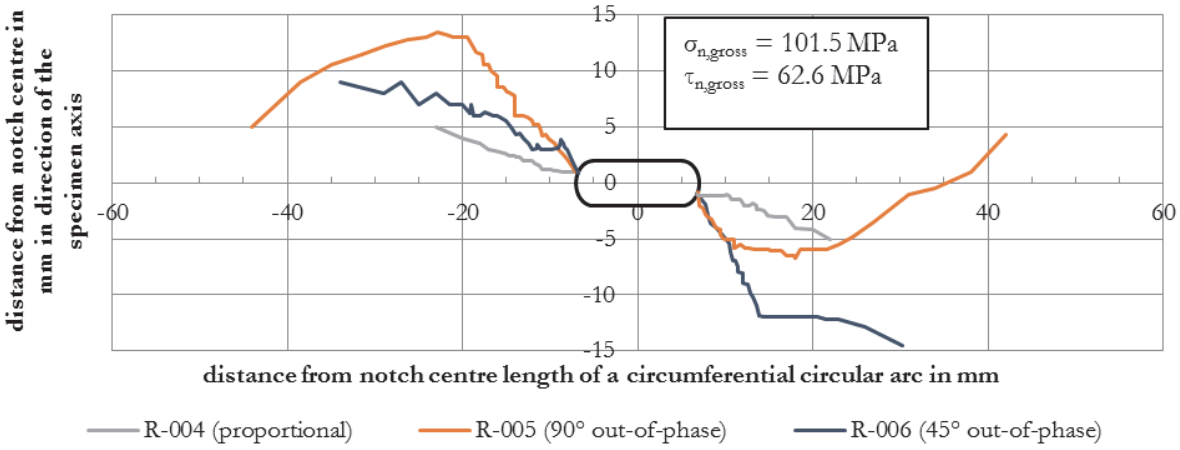

Figure 8: Crack growth curves of specimens R-004, R-005 and R-006 with F_{max} = 33 kN, M_{max} = 382 Nm and $R_F = R_M$ = -1

THE CRACK GROWTH SIMULATION

Multiaxial Loading - Proportional Loading

Under the light of the data taken from the real experiments, linear elastic simulations have been done on ABAQUS for the experiment R-004. The data concerning the position of the crack tip was already available. As previously been postulated, a significant portion of shear mode (about %20 of the opening mode) was observed among both cracks. Fig. 9 and 10 9 depict the growth of the stress intensity factors with the crack length.

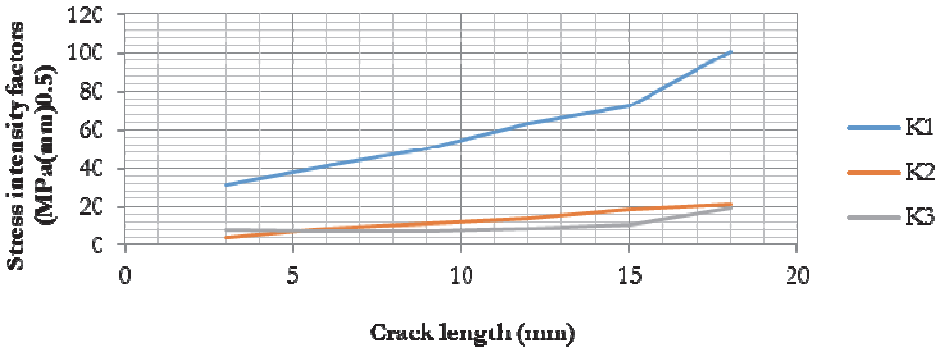

Figure 9: Stress intensity factors in specimen R-004, crack 1 proportional loading with F_{max} = 33 kN, M_{max} = 382 Nm, $R_F = R_M$ = -1, steel S235.

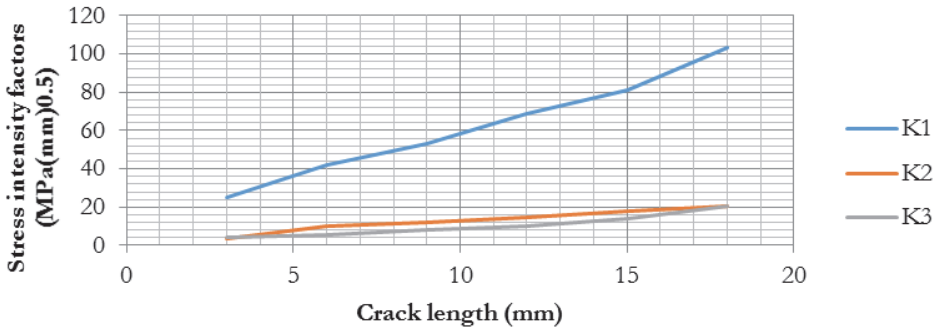

Figure 10: Stress intensity factors in specimen R-004, crack 2 proportional loading with F_{max} = 33 kN, M_{max} = 382 Nm, $R_F = R_M$ = -1, steel S235.

CONCLUSION

Fatigue crack growth under non-proportional loading cases lead to crack paths, which are not understood fully. A collection of results was presented in this paper. A number of conclusions can be derived from these results:

- The assumption of planar symmetrical crack growth in axial specimens is quite plausible, in spite of bending effects. In [20], another similar experiment with a larger load was discussed and simulated. A change in crack path because of the bending load, which increases with increasing crack length, was not observed.
- The crack that was loaded proportionally undergoes a non-negligible shear mode (about %20), as the crack growth pattern with zigzags suggest. A final conclusion, why the crack sees this as a second option is though not clear.
- A general tendency for cracks under non-proportional loadings is difficult to derive from the morphology. However, DIC [19] and FE-simulations (ongoing) can lead to some important conclusions. Such simulations can be compared with the DIC results in [19] and a clearer answer for this alternating crack growth pattern might be found.

ACKNOWLEDGEMENTS

The German Research Foundation (Deutsche Forschungsgemeinschaft) is greatly acknowledged by the authors for financial support under grant Vo729/13-1.

REFERENCES

[1] Zerres, P., Vormwald, M., Review of fatigue crack growth under non-proportional mixed-mode loading, Int. J. Fatigue, 58 (2014) 75-83.
[2] Qian, J., Fatemi, A., Mixed mode fatigue crack growth: a literature survey, Eng. Fract. Mech., 55(6) (1996) 969-990
[3] Highsmith, J., PhD Thesis, Georgia Institute of Technology, USA, (2009).
[4] Richard, H.A., Fulland, M., Sander, M., Theoretical crack path prediction, Fatigue Fract. Eng. Mater. Struc., 28 (2005) 3-12
[5] Roberts, R., Kibler, J., Mode II fatigue crack propagation, J. Basic Eng., 93D (1971) 671-680
[6] Tanaka, K., Fatigue crack propagation from a crack inclined to the cyclic tensile axis, Eng. Fract. Mech., 6 (1974) 493-507
[7] Brown, M.W., Miller, K.J., Initiation and growth of cracks in biaxial fatigue, Fatigue Fract. Eng. Mater. Struc., 1 (1979) 231-246.
[8] Otsuka, A., Tohgo, K., Fatigue Crack Initiation and Growth Under Mixed Mode Loading in Aluminum Alloys 2017-T3 and 7075-T6, Eng. Fract. Mech., 28 (1987) 721-732.
[9] Socie, D.F., In: Fatigue 87, proc. 3rd int. conf. fatigue and fatigue thresholds, 2 (1987) 599-616,.
[10] Doquet, V., Bertlino, G., Local approach to fatigue cracks bifurcation, Int. J. Fatigue, 30 (2008) 942-950
[11] Hoshide, T., Socie, D.F., Mechanics of mixed mode small fatigue crack growth, Eng. Fract. Struc., 26 (1987) 841-850.
[12] Savaidis, G., Seeger, T., Consideration of multiaxiality in fatigue life prediction using the closure concept, Fatigue Fract. Eng. Mater. Struc., 20 (1997) 985-1004.
[13] Döring, R., Hoffmeyer, J., Seeger, T., Vormwald, M., Short fatigue crack growth under nonproportional multiaxial. elastic-plastic strains, Int. J. Fatigue, 28 (2006) 972-982.
[14] Hertel, O., Vormwald, M., Short-crack-growth-based fatigue assessment of notched components under multiaxial variable amplitude loading, Eng. Fract. Mech. 78 (2011) 1614-1627.
[15] Hertel, O., Vormwald, M., Multiaxial fatigue assessment based on a short crack growth concept, Theor. Appl. Fract. Mech., 73 (2014) 17-26.
[16] Dowling, N.E., Begley, J.A., Fatigue crack growth during gross plasticity and the J-integral, ASTM STP 590 (1976) 82-103.
[17] Wüthrich C., The Extension of the J-Integral Concept to Fatigue Cracks, Int. J. Fract., 20 (1982) R35-7.
[18] Hertel, O., Döring, R., Vormwald, M., Cyclic J-integral under nonproportional loading, Proc. 7th Int. Conf. Biaxial/Multiaxial Fatigue Fract. (2004) 513-518.
[19] Hos, Y., Freire, J.L.F., Vormwald, M., Measurements of strain fields around crack tips under proportional and non-proportional mixed-mode fatigue loading, Int. J. Fatigue (2016) (in press).

[20] Hos Y, Vormwald M., Experimental study of crack growth under non-proportional loading along with first modeling attempts, Int J Fatigue (2016) (in press).
[21] Zerres, P., Brüning, J., Vormwald, M., Risswachstumsverhalten der Aluminiumlegierung ALMg4.5Mn unter proportionaler und nichtproportionaler Schwingbelastung, Mater. Test., 53 (2011) 109-117.
[22] Zerres, P., Brüning, J., Vormwald, M., Fatigue crack growth behavior of fine-grained steel S460N under proportional and non-proportional loading, Eng. Fract. Mech., 77 (2011) 1822-1834.
[23] Hos, Y., Vormwald, M., Freire, J.L.F., Using digital image correlation to determine mixed mode stress intensity factors in fatigue cracks, Proceedings of COTEQ 2015, Conference on Technology of Equipment, organized by ABENDI, Brazilian Society for NDT and Inspection, June, 2015.
[24] Vormwald, M., Fatigue Crack Propagation under Large Cyclic Plastic Strain Conditions, Procedia Mater. Sc. 3 (2014) 301-306
[25] Vormwald, M., Hos, Y., Freire, J.L.F., Measurement and simulation of strain fields around crack tips under mixed-mode fatigue loading, Frattura ed Integrita Strutturale, 33 (2015) 42-55.
[26] Hos, Y., Vormwald, M., Measurement and simulation of crack growth rate and direction under non-proportional loadings, Frattura ed Integrita Strutturale, 34 (2015) 133-141.